Available online at www.sciencedirect.com

ScienceDirect

IFAC PapersOnline CONFERENCE PAPER ARCHIVE

IFAC PapersOnLine 55-9 (2022) 70–75

Evaluation of the Symmetrically Switched Converter Structures on the Frequency Regulation of Standalone Micro Hydro Power Plants

H. Bory*, L. Vazquez*, H. Martínez, Y. Majanne*****

**Electrical Engineering Faculty, University of Oriente, Ave. Las Americas s/n, 90400 Santiago of Cuba, Cuba (e-mail: bory@uo.edu.cu, lvazquez@uo.edu.cu, lvazquez0211@gmail.com)*

*** Departamento de Ingeniería Electrónica, Escuela de Ingeniería de Barcelona Este (EEBE), Universidad Politécnica de Cataluña (UPC) – BarcelonaTech, Av. De Eduard Maristany, nº 10 – 14, E-08019, Barcelona, España (e-mail: herminio.martinez@upc.edu)*

**** Faculty of Engineering and Natural Sciences, Tampere University, P.O. Box 541, FI-33014 Tampere University, Finland (e-mail: yrjo.majanne@tuni.fi))*

Abstract: Micro hydro power plants (μHPP) are typically used to supply electric energy to microgrids outside the national power grids taking care of the frequency control of the isolated system. A conventional way to maintain the load balance in the system is to use thyristor switched AC-AC converters controlled dump loads. A disadvantage of the AC-AC converters is their reactive power consumption decreasing the power factor at the generator output. To avoid this problem the authors have earlier proposed two converter topologies utilizing symmetrical switching scheme resulting to zero reactive power consumption. The objective of this paper is to evaluate the frequency regulation loop performance of the dump load controlled single generator system by using the symmetrically switched converter structures. Evaluation is carried out by analyzing the performances of different converter structures in a simulator representing the operation of a Cuban μHPP "Los Gallegos". The results showed that the frequency regulation loop performance using each proposed converter structure satisfied the Cuban standard of frequency regulation, but with the symmetrically switched structures reactive power consumption was reduced resulting to reduced losses and improved effective current delivery capacity of the generator.

Keywords: frequency regulation, symmetrical switching, dump load.

1. INTRODUCTION

Small capacity micro hydro power plants (μHPP) are often located in remote areas without connection to a national power grid and supplying isolated mini-grids as only generators. In those isolated single generator systems, the μHPP is responsible to maintain the system frequency and voltage. A common way to realize the power balance control in this kind of system is a dump load control, where the turbine generator set is running as an uncontrolled run-of-the-river hydro power plant, and the supply-demand balance of the system is maintained by a load control of an additional resistive load immersed in the running water. Conventionally the power control of the dissipating dump load resistors is carried out by thyristor switched AC-AC converters (Kurtz *et. al.*, 2005; Bory, 2011; Adhikari *et al*., 2013; Peña *et al.*, 2013; Guillermo & Leonardo, 2016; Salhi, *et al*., 2016; Fong *et al*., 2018; Hussnain, *et al*., 2018; Peña & Wong, 2020).

One disadvantage of this kind of AC-AC converter is a reactive power consumption as a function of the triggering angle of the thyristor. Reactive power consumption degrades the power factor at the output terminals of the generator and hence decreases the generator current supply capability. Excessive reactive power consumption in the system increases generator losses and may also result to operation beyond the capacity curve of the generator resulting to voltage instability and overheating of the generator.

As a solution for this problem, Bory *et al*. 2019 proposed two rectifier structures controlled by symmetrically switched IGBT switches. The basic idea of the symmetrical switching is to switch the half-wave symmetrically around the peak voltage angle so that the net reactive power generated by the switching process during the half-wave is zero. The research question of this paper is: What is the performance of these symmetrically switched converters on the frequency control loop of the single μHPP supplied mini-grid? The research question is studied by simulating the operation of Los Gallegos μHPP in Cuba with three different control loop structures; phase specific asymmetrically switched thyristor controlled AC-AC converters, symmetrically switched IGBT controlled three-phase converter, and phase specific symmetrically switched IGBT controlled converters.

In Chapter 2 dynamic models of simulated components and topologies of analyzed converters are introduced. Chapter 3 introduces a MatLab/Simulink model of the Los Gallegos case μHPP process including the power system components and the control loop. In chapter 4 the frequency control loop performances using different converter structures are evaluated, and finally chapter 5 concludes the results.

10.1016/j.ifacol.2022.07.013

2. MODEL OF THE FREQUENCY REGULATION LOOP

Fig. 1 shows the structural block diagram of the µHPP supplied mini-grid system. Kinetic energy of running water is converted to mechanical energy in a hydraulic turbine. Next the mechanical energy is converted to electric energy in a generator connected with the turbine, and electric power is supplied to consumption via mini-grid. The total load consists of the variable end user load and controllable dump load.

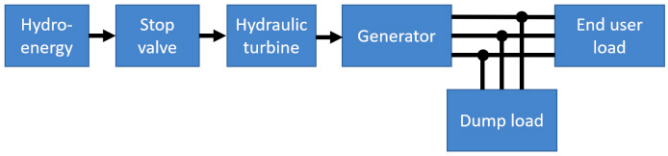

Figure 1. Functional diagram of the µHPP.

2.1 *Hydraulic Turbine*

Mechanical power (P_m) generated by the hydraulic turbine is

$$P_m = \eta_t \rho g Q_V H_n \tag{1}$$

where η_t is the turbine efficiency [-], ρ is water density [kg/m^3], g is gravity constant [m/s^2], Q_V is water flow rate [m^3/s], and H_n is the net head [m]. (Carta, et al., 2009; Rashid, 2016)

2.2 *Generator Mechanical Part*

In a single generator system the frequency of the system is defined just by the rotation speed of the generator, and the rotor is all the time synchronized with the stator frequency. Thus, any damper system is not needed in the model. (Bory *et al*., 2021)

The momentum balance equation applied to the turbine generator system is:

$$J_T \frac{d}{dt} w_{rm} = T_M - T_G - T_F \tag{2}$$

where J_T is a total inertia of the turbine-generator [kgm^2], T_M turbine rotor mechanical torque [Nm]. T_G generator electrical torque [Nm], T_F total torque of the turbine and generator aerodynamic drag [Nm], w_{rm} generator rotor speed [rad/s].

T_F is defined as $T_F = K_F w_{rm}$, where K_F is the drag coefficient [Nms/rad].

Multiplying both sides of Eq. (2) by w_{rm}, it is obtained:

$$J_T w_{rm} \frac{d}{dt} w_{rm} = P_M - P_G - K_F w_{rm}^2 \tag{3}$$

where P_M is a turbine mechanical power [W], and P_G generator electrical power [W].

Next the nonlinear Eq. (3) is linearized in the operation point P_{M0} and P_{G0} at the nominal rotation speed, w_{rm0}. The system variables in the neighborhood of the operation point can be written as:

$$\begin{aligned} w_{rm} &= w_{rm0} + \Delta w_{rm} \\ P_M &= P_{M0} + \Delta P_M \\ P_G &= P_{G0} + \Delta P_G \end{aligned} \tag{4}$$

Substituting process variables of Eq. (3) by Eq. (4), and recognizing that at the steady state in the operation point $P_{Mo} - P_{Go} - K_F w_{rmo}^2 = 0$, and ignoring second order terms of increments $\Delta(.)$, it is obtained:

$$J_T w_{rmo} \frac{d}{dt} \Delta w_{rm} + 2K_F w_{rmo} \Delta w_{rm} = \Delta P_M - \Delta P_G \tag{5}$$

Increment of the generator power P_G equals with the sum of increments of user load P_U and dump load P_L, $\Delta P_G = \Delta P_U + \Delta P_L$. Moreover, $w_{rm} = {4\pi f}/{P}$ and $w_{rmo} = {4\pi f_o}/{P}$, where P is the number of the generator poles, f is the actual system frequency and f_0 = 60 Hz. Acknowledging these notations, Eq. (5) is rewritten in:

$$J_T \left(\frac{4\pi}{P}\right)^2 f_o \frac{d}{dt} \Delta f + 2\left(\frac{4\pi}{P}\right)^2 f_o K_F \Delta f = \Delta P_M - \Delta P_U - \Delta P_L \tag{6}$$

Laplace transformation of Eq. (6) is:

$$\Delta F(s) = \frac{\dfrac{P^2}{2(4\pi)^2 f_o K_F}}{\dfrac{J_T}{2K_F} s + 1} \left[\Delta P_M(s) - \Delta P_U(s) - \Delta P_L(s)\right] \tag{7}$$

From Eq. (7) it can be defined the following constants between the system powers and the frequency: Generator gain $K_G = P^2/\{2(4\pi)^2 f_o K_F\}$, [Hz/W], and turbine-generator mechanical time constant $T_G = J_T/(2K_F)$, [s]. (Bory *et al*., 2021)

2.3 *Dynamic Models of the Two Rectifiers with Symmetrical Switching and the AC-AC Converter*

Figure 2 shows the structures of the symmetrically switched three phase rectifier (a), and the single phase rectifier (b). In the three-phase rectifier structure, the excessive power is dissipated in a single dump load resistance, but in the single-phase rectifier structure, every phase has its own controllable converter and a dump load. In the Figure 2 (c) is shown the structure of the AC-AC converter and the dump load.

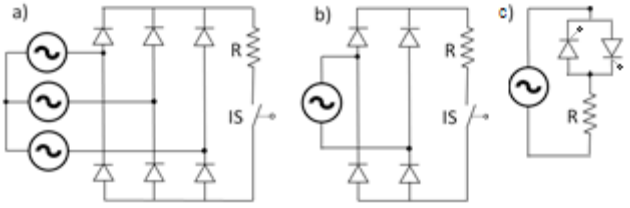

Figure 2. Structures of the symmetrically switched three-phase rectifier a), and the single-phase rectifier b) and c) structure of the AC-AC converter.

The mathematical expression of the power at the input of the converter (P_L) as a function of the control voltage (M) related to the switching angle of the converter using the step function u, is:

$$P_L(t) = K_C u\left(t - T_C\right) M(t) \tag{8}$$

where Tc is the average delay from the control signal $M(t)$ change to the response of the dump load power consumption $P_L(t)$. The gain Kc is determined as $K_c = \Delta P_L/\Delta M$. The Laplace transformation of the Eq. (8) is:

$$P_L(s) = K_C e^{-T_C s} M(s) \tag{9}$$

Approximating the delay term by a first order lag and applying incremental variables Δ (.), the transfer function from control signal change ΔM to dump load power consumption change ΔP_L is given by:

$$\frac{\Delta P_L(s)}{\Delta M(s)} = \frac{K_C}{T_C s + 1} \tag{10}$$

(Dewan, 1986) has shown that for three phase systems Tc is approximately equal to 0.001 s. In this study Eq. (10) is applied as a transfer function of the set of three thyristor-controlled AC-AC converters.

3. SIMULATION MODEL AND CASE SYSTEM

Figure 3 represents the MatLab/Simulink model implemented to evaluate the performances of different converter structures on the frequency regulation loop of the μHPP supplied single generator mini-grid.

The main components of the model are: the hydraulic turbine model, Eq. (1); measurement blocks for efective voltage and current, active, reactive and apparent powers and power factor connected with different system components; the enduser load modelled as a three-phase series RL load; converters modelled according to the component models applied in this research. The electrical part of the generator is modelled by a Three-Phase Programmable Voltage Source; The proportional integral (PI) frequency controller is modelled by a transfer function $Gcf(s)$; the mechanical part of the generator is modelled according to Eq. (7).

Case system representing the real μHPP and mini-grid system is a Los Gallegos μHPP in Cuba. The parameters of the Los Gallegos power system are as follows: rated power of the turbine-generator set 12.0 kW, generator phase voltage 110 V RMS, nominal frequency 60 Hz, generator speed 1200 rpm (6 poles), rotor friction coefficient 0.0063 Nms/rad (aerodynamic drag), and the total inertia moment of the turbine-generator set 7.60 kgm^2. Operation range of the frequency measurement is from 55 to 65 Hz giving an output voltage from 0 to 10 V. Power consumed by end-users varies from 3.0 kW to 12.0 kW.

The applied PI type frequency controller is tuned by applying a pole assignment method according to frequency quality requirements defined in the Cuban standard (NC62-04) for frequency stability. The requirements state that the maximum allowed steady state error of the rated frequency is 1%, the maximum deviation during the transients must be less or equal than ± 1 Hz, and the settling time of the system frequency must be less than 5 s.

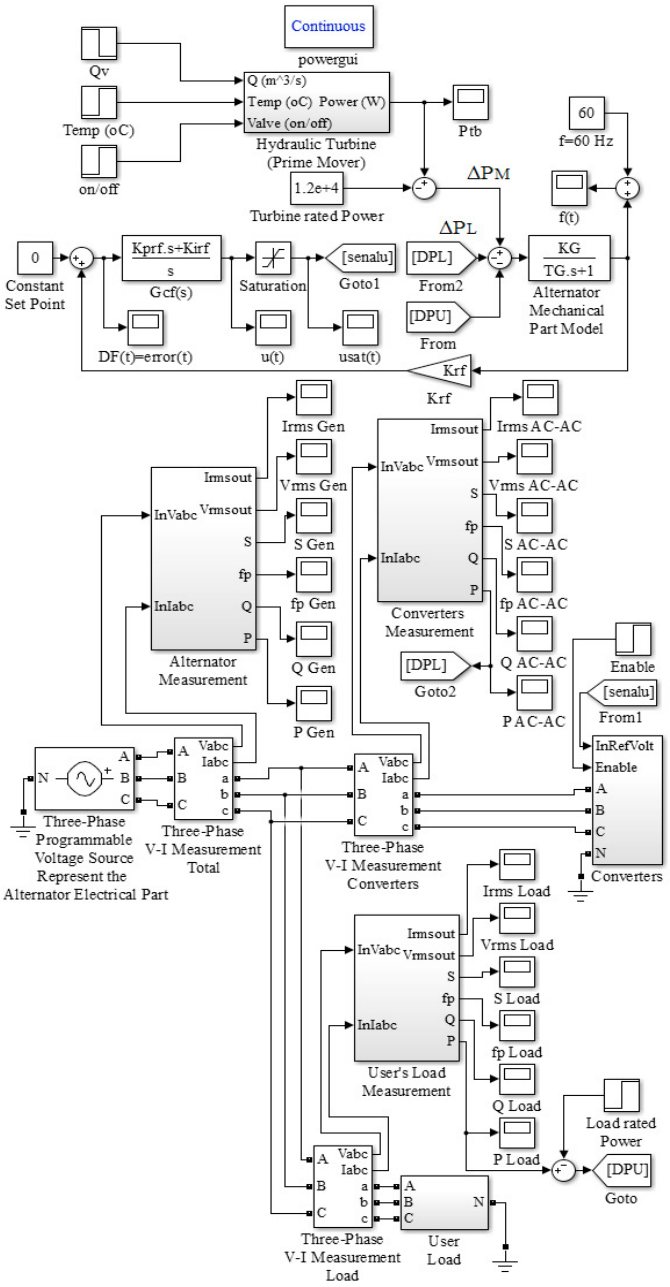

Figure 3. MatLab/Simulink model applied in the performance analysis of the frequency control of mini-grids.

Those requirements are fulfilled by choosing a damping ratio (ξ) of 0.707, and an undamped natural frequency (w_n) of 10 rad/s. The controller parameters for proportional and integral gains K_{prf} and K_{irf} are:

$$K_{prf} = \frac{2\xi w_n T_G - 1}{K_C K_G K_{rf}} = 11.79, \quad K_{irf} = \frac{w_n^2 T_G}{K_C K_G K_{rf}} = 83.35\ s^{-1}$$

where: K_C = (12 000 W – 3 000 W)/5V = 1 800 W/V (maximum dump load P_{CMAX} is 9.0 kW and control signal range is 0 – 5 V), generator gain K_G=0.3 Hz/W, and turbine generator mechanical time constant caused by the aerodynamic drag T_G = 600.1 s, and gain from measured frequency to transmitter signal

$$K_{rf} = \frac{U_{rfmáx} - U_{rfmín}}{F_{máx} - F_{mín}} = \frac{10\,V - 0\,V}{65\,Hz - 55\,Hz} = 1\,V/Hz\,.$$

4. EVALUATION OF THE FREQUENCY CONTROL LOOPS

Operation performances of the symmetrically switched three-phase converter and the three separate symmetrically switched single phase converters are compared with the performance of the existing thyristor controlled phase-specific AC-AC converters.

The performance of each converter structure as a part of the frequency control loop is evaluated by analyzing closed loop responses during step changes of the user load. The evaluation criteria are chosen from the Cuban standard (NC62-04). The test sequence follows typical user load changes in Los Gallegos mini-grid. Dominating load changes in the system varies between 3 – 4 kW. At a time instant t = 3.0 s. the active power consumption is reduced from nominal load by 3.0 kW and reactive power consumption by 2.5 kVAR. At t = 5.0 s. the active power consumption is reduced by another 3.0 kW and reactive power consumption by 3.0 kVAR. At t = 6.5 s the active power consumption is increased by 4.0 kW and reactive power consumption by 3.5 kVAR.

4.1 Thyristor controlled AC-AC converters

Figure 4 shows the closed loop control error and system frequency behavior during the load change sequence with the conventional AC-AC converter controlled dump load. The maximum deviation of the frequency from its rated value is less than 0.1 Hz (1 V = 1 Hz), which is well below the required 1 Hz, and the steady state error is zero. Also, the settling time of the frequency transient after the load change is well below the 5 s. Thus, the requirements of the standard NC62-04 are fulfilled.

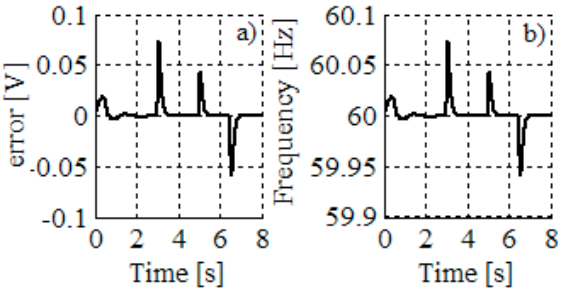

Figure 4. Closed loop response of a) the control error and b) the actual frequency controlled by the phase specific thyristor controlled AC-AC converter.

Upper graphs of Figure 5 show the time responses of the reactive powers of the generator, Q_{Gen}, the set of AC-AC converters, $Q_{AC\text{-}AC}$, and the end-user load, Q_U. Lower graphs show the power factors fp_{Gen}, $fp_{AC\text{-}AC}$, and fp_U respectively. Signals are measured from the generator output terminals, the input terminals of the set of three AC-AC converters, and the end-user´s load.

The graphs show that the generator must supply more reactive power, Q_{Gen}, than what is the reactive power consumption of the end-user load, Q_u.

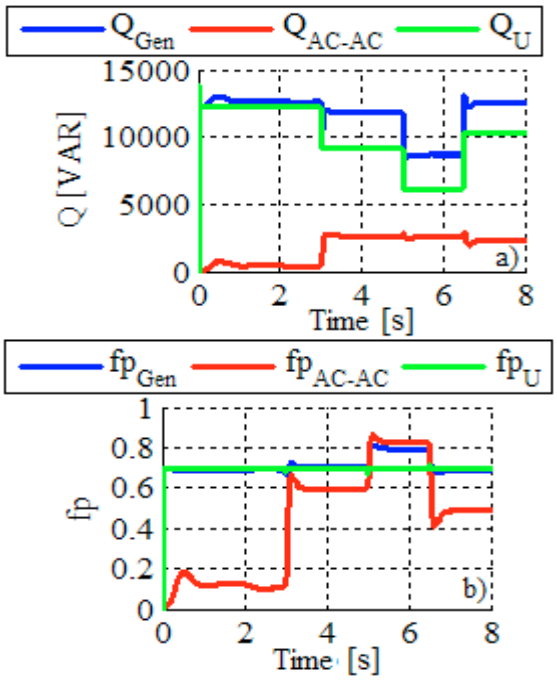

Figure 5. Time responses of the reactive powers Q and power factors fp of the generator, the set of AC-AC converters, and the end-user load.

This is because of the reactive power consumption $Q_{AC\text{-}AC}$ in the AC-AC controlled dump load system. As a result, even if the system frequency is regulated satisfactorily with the AC-AC converters, their reactive power consumption impairs the generator's operation capacity.

4.2 Three-phase symmetrically switched converter

Figure 6 shows the frequency control loop performance for the three-phase symmetrically switched converter structure (Figure 2a). The maximum deviation of the frequency from its rated value is less than 0.1 Hz, the steady state error is zero, and frequency settling time after the load change is lesser than 5 s. Thus, the requirements set for the system frequency stability in the standard NC62-04 are fulfilled.

Figure 7 shows the time responses of the reactive powers Q and power factors fp of the generator, the three phase symmetrically switched converter, and the end-user load.

Now the generator must supply reactive power, Q_{gen}, only equal to the end-users' reactive power consumption Q_u. This is because the reactive power consumption of the dump load controlled symmetrically switched tree phase converter is zero.

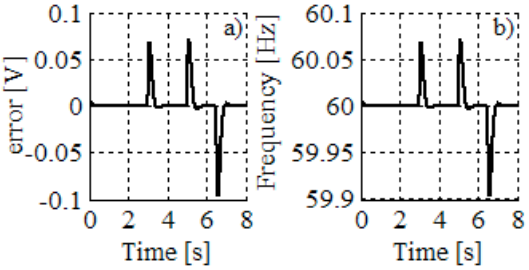

Figure 6. Closed loop behaviour of the control error, a), and the actual frequency, b), of the symmetrically switched three phase converter.

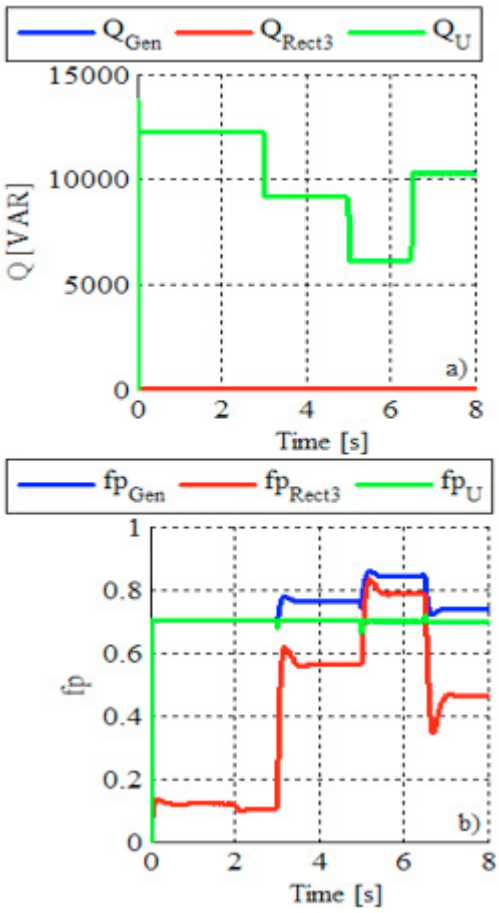

Figure 7. Time responses of the reactive powers *Q* and power factors *fp* of the generator, three phase symmetrically switched converter, and the end-user load.

Figure 8 shows effective currents of one generator phase connected with the AC-AC converter, $Irms_{GenAC\text{-}AC}$, and with the symmetrically switched three-phase converter, $Irms_{GenRect3}$. Figure shows that $Irms_{GenRect3}$ is smaller compared with $Irms_{GenAC\text{-}AC}$. The maximum difference is 4 A.

4.3 Three single-phase symmetrically switched converters

Figure 9 shows the frequency error signal and the instantaneous system frequency of the configuration with three single phase

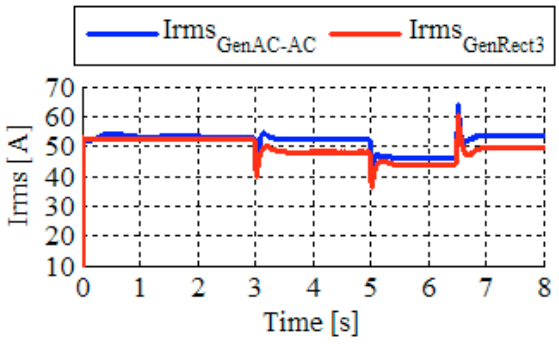

Figure 8. Effective phase currents supplied by the generator connected with the set of three AC-AC converters and the symmetrically switched three-phase converter.

symmetrically switched converters (Figure 2b). The maximum frequency error is less than 0.1 Hz, the steady state error is zero, and the settling time after the load change is less than 5 s. Thus, the frequency stability requirements set by the national standard NC62-04 are fulfilled.

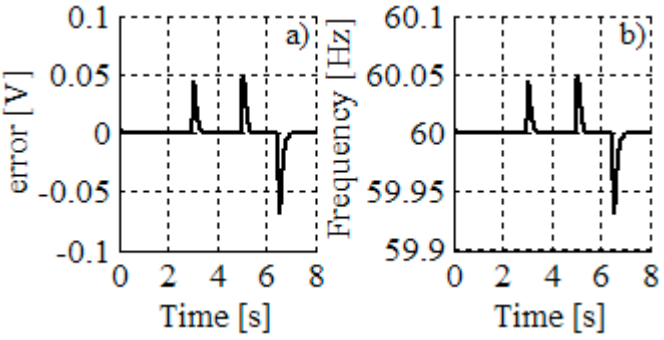

Figure 9. Closed loop behaviour of the control error, a), and the actual frequency, b), of the three symmetrically switched single phase converters.

Figure 10 depicts the time behavior of the reactive powers *Q* and power factors *fp* with single phase symmetrically switched converters. Also in this case the generator must supply a reactive power, Q_{gen},, only equal to Q_u, and the power factor in the generator output terminal is improved compared with the AC-AC case.

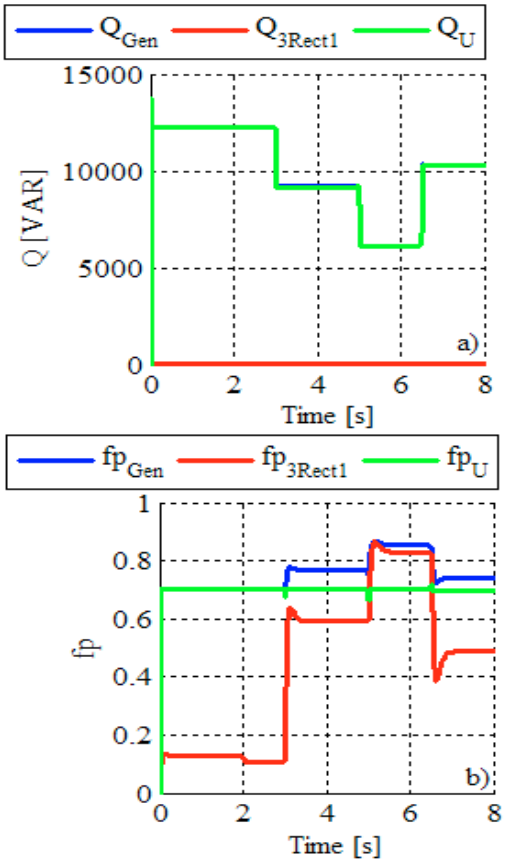

Figure 10. Time responses of the reactive powers *Q* and power factors *fp* of the generator, three single phase symmetrically switched converters, and the end-user load.

Figure 11 shows effective generator phase currents connected with the thyristor controlled AC-AC converters, $Irms_{GenAC-AC}$, and with the set of symmetrically switched single-phase converters, $Irms_{Gen3Rect1}$. The maximum difference between the currents is 4.5 A.

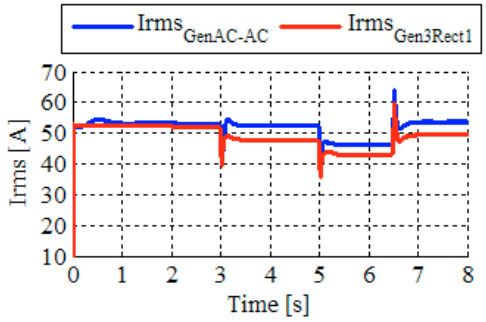

Figure 11. Effective currents supplied by the generator connected with the conventional AC-AC converter and the symmetrically switched single phase converters. (Bory *et al*., 2021).

As a brief remark, in this paper was used the following *fp* definition under nonsinusoidal current condition:

$$fp = \frac{I_{rms1}}{I_{rms}} \cdot \cos(\theta_{V1}) \tag{11}$$

where: I_{rms1} is the effective value of the current first harmonic, I_{rms} is the effective current and θ_{V1} is the phase angle between the line to grown voltage and the current first harmonic.

For the cases of the three-phase and single-phase symmetrically switched converters $\theta_{V1}=0$, but $fp<1$ due to $I_{rms1}< I_{rms}$.

5 CONCLUSIONS

The results show that with the proposed converter structures controlled by symmetrical switching satisfy the requirement impose by the NC62-04 on frequency regulation. Also the power factor at the output terminal of the generator and the current supply capacity of the generator are improved.

ACKNOWLEDGEMENTS

This contribution is a result of the Power Electronics Control in Energy and Motion Systems group (PECEM) from University of Oriente, Santiago de Cuba. The work was supported by EU's Erasmus+ programme CRECE (Capacity Building for Renewable Energy Planning in Cuban Higher Education Institutions) and the IRIS project (Cuban energy transformation. Integration of Renewable Intermittent Sources in the power system) financed by the Academy of Finland, Grant/Award Number 320229. The authors of the article gratefully acknowledge the financers and project partners.

REFERENCES

Adhikari R. et al. (2013). Improved Electronic Load Controller for Three Phase Isolated Micro-Hydro Generator. Kathmandu: Fifth International Conference on Power and Energy Systems.

Bory, H., (2011), Metodología para el mejoramiento del factor de potencia en Pequeñas Centrales Hidroeléctricas en régimen autónomo y que emplean convertidores de CA en CA para la regulación de frecuencia. Master Work. Automation Department. Electrical Engineering College. University of Oriente. Cuba.

Bory H., Vazquez L., Martínez H., Majanne Y. (2019). Symmetrical Angle Switched Single Phase and Three Phase Rectifiers: Application to Micro Hydro Power Plants. ScienceDirect 52-4, 216-21.

Bory H., Martin J. L., Martinez I., Vazquez L. (2021). Effect of Symmetrically Switched Rectifier Topologies on the Frequency Regulation of Standalone Micro-Hydro Power Plants. Energies 14, 3201.

Carta J., Colmenar A., Castro M., (2009). *Centrales de energías renovables. Generación eléctrica con energías renovables* (M. Martín-Romo Ed. ed.). s.l.:Pearson Educación, S.A.

Dewan, S., Slemon, G. & Straughen, A., (1986). *Power Semiconductor Drives*. Primera Edicion Cubana ed. s.l.:Edición Revolucionaria.

Fong J. et al. (2018). Design of a regulator of frequency, for small central hydroelectric in isolated operation**.** Journal of Engineering and Technology for Industrial Applications. DOI: https://dx.doi.org/10.5935/2447-0228.20180021.

Guillermo, C., Leonardo, O. Implementación de un controlador PI digital en un Controlador Electrónico de Carga con estrategia de regulación mixta para regular la frecuencia en una Micro-central Hidroeléctrica. XXVI Jornadas En Ingeniería Eléctrica Y Electrónica – EPN. Available online: http://bibdigital.epn.edu.ec/bitstream/15000/17216/1/2016AJIEE-27.pdf [Consulted: 13-01-2016]

Hussnain M. et al. (2018). Micro Hydro Power Plant Dummy Load Controller. s.l.:IEEE.

Kurtz, V., Anocivar, H., (2005). Sistema Mixto para el control de la Generación en Micro Centrales Hidroeléctricas. XI ELPAH. Encuentro Latinoamericano y del Caribe sobre Pequeños Aprovechamientos Hidroenergéticos.

Peña, L., Dominguez, H., Fong, J., Garcia, J., Alzórris, P., Regulación de frecuencia en una Minihidrolectrica por carga lastre mediante un pc Embebido. Universidad Politécnica de Cataluña. Available online: http://www.aedie.org/9CHLIE-paper-send/291-PE%D1A.pdf. [Consulted: 12-06-2013]

Peña L. & Fariñas E., (2020). Mejoras en la eficiencia energética de las micro-hidroeléctricas aisladas mediante la regulación combinada flujo-carga lastre. Ingeniería Energética 41, 1-11.

Rashid, M., (2016). *Electric Renewable Energy Systems.* Florida: Academic Press.

Salhi, I., Doubabi, S., Essounbouli, N. & Hamzaoui, A., (2016). Frequency regulation for large load variations on micro-hydro power plants with realtime implementation. Int. Journal Electric Power Energy System 60, 6-13.